

Macrocyclic Polyphosphane Ligands: Cobalt(II) and Nickel(II) Complexes of 1,10-Dipropyl-4*RS*, 7*SR*, 13*SR*, 16*RS*-Tetraphenyl-1,10-Diaza-4,7,13,16-Tetraphospha-cyclooctadecane and Crystal Structure of the Cobalt Tetraphenylborate Monohydrate Complex

STEFANO MANGANI, PIERLUIGI ORIOLI

Istituto di Chimica Generale, Università di Siena, Via Pian dei Mantellini 44, 53100 Siena, Italy

MARIO CIAMPOLINI*, NICOLETTA NARDI

Dipartimento di Chimica, Università di Firenze, Via J. Nardi 39, 50132 Florence, Italy

and FABRIZIO ZANOBINI

ISSECC (C.N.R.), Via D. M. Guerrazzi 27, 50132 Florence, Italy

Received August 2, 1983

The X-ray crystal structure of the title compound has been carried out. The crystals are triclinic, space group $P\bar{1}$, $a = 13.252(2)$, $b = 13.943(2)$, $c = 24.316(5)$ Å, $\alpha = 70.660(14)$, $\beta = 75.219(14)$, $\gamma = 69.231(13)^\circ$ for $Z = 2$. The structure has been refined to an R factor of 0.069 by the least-squares technique. The cobalt atom is five-coordinated by the four phosphorus atoms of the macrocycle and by a water molecule forming a distorted square-pyramidal geometry. The stereochemistry of some cobalt(II) and nickel(II) complexes of the same ligand were investigated, in the solid state and in solution, by electronic spectroscopy.

Introduction

In a continuing study of the coordination behaviour of macrocyclic ligands we have reported the synthesis and the complex formation of macrocycles of type I (Fig. 1), $[18]aneP_4E_2$, which contain four phosphane groups and two different donor atoms ($E = O, S, N-Pr$) [1–6]. These compounds occur as five diastereoisomers, stable at room temperature, which exhibit a markedly different coordinative behaviour in their cobalt(II) and nickel(II) complexes. Thus, with the macrocycle $[18]aneP_4O_2$, both of the β -

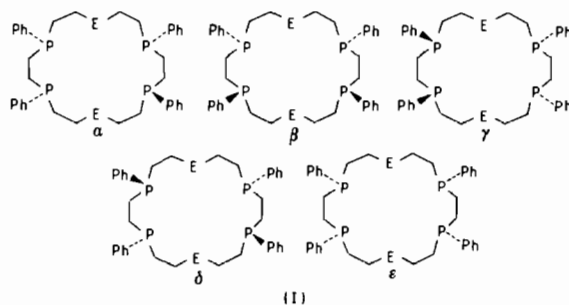


Fig. 1. The five diastereoisomers of $[18-aneP_4N_2]$.

and δ -isomers give *trans*-octahedral cobalt(II) complexes with facial [1] and meridional [2] arrangements of the $P \cdots O \cdots P$ moieties, respectively. On the contrary, a square pyramidal geometry is exhibited by $[Co(\alpha-[18]aneP_4O_2)]^{2+}$ [1] and a square-planar one by $[Ni(\epsilon-[18]aneP_4O_2)]^{2+}$ [6]. Such a behaviour has been rationalised in terms of the mutual chiralities of the phosphane groups in the $P \cdots O \cdots P$ chains. On the other hand, δ -[18]- $aneP_4S_2$ gives cobalt(II) and nickel(II) complexes with trigonal-bipyramidal structure, one sulphur atom being uncoordinated [5]. This has been related to the higher donor strength of thioether sulphur compared to the ethereal oxygen, which disfavors octahedral coordination for d^7 (low-spin) and d^8 electron configurations.

*Author to whom correspondence should be addressed.

As far as the [18]aneP₄N₂ macrocycle is concerned, we have reported the X-ray structure determination of [Ni(γ -[18]aneP₄N₂)] [BPh₄]₂, where the γ isomer has 4*RS*, 7*SR*, 13*SR*, 16*RS* configuration of the chiral phosphane groups [3]. We describe here the X-ray crystal determination of [Co(H₂O)(γ -[18]aneP₄N₂)] [BPh₄]₂ and the coordination behaviour of some cobalt(II) and nickel(II) derivatives of the same diastereoisomer.

Experimental

Ligand Synthesis

The ligand was prepared by the method previously described [3].

Preparation of Complexes

$MBr_2 \cdot \gamma[18]aneP_4N_2 \cdot nH_2O$ ($n = 1$ and 0 for $M = Co$ and Ni , respectively)

A solution of MBr₂ (0.1 mmol) in 7 ml of 1:1 (v/v) ethanol/water was added to a solution of the ligand (0.1 mmol) in 20 ml of ethanol. The resulting solution was evaporated to about 5 ml and 15 ml of water was added dropwise. On standing overnight, crystals separated which were filtered off, washed with 1:5 (v/v) ethanol/water, and dried *in vacuo*. *Anal.* Found: C, 53.1; H, 6.4; N, 3.1. *Calcd.* for C₄₂H₆₀Br₂N₂OP₄Co: C, 53.01; H, 6.36; N, 2.94%. Found: C, 53.9; H, 6.2; N, 3.0. *Calcd.* for C₄₂H₅₈Br₂N₂P₄Ni: C, 54.05; H, 6.26; N, 3.00%.

$M[BPh_4]_2 \cdot \gamma[18]aneP_4N_2 \cdot nH_2O$ ($n = 1$ and 0 for $M = Co$ and Ni , respectively)

A solution of M(BF₄)₂·6H₂O (0.1 mmol) and Na(BPh₄) (0.3 mmol) in 7 ml of ethanol was added to a solution of the ligand (0.1 mmol) in 20 ml of acetone. The resulting solution was evaporated to about 10 ml and a few drops of water were slowly added. The precipitate was filtered off, washed with ethanol and dried *in vacuo*. *Anal.* Found: C, 75.7; H, 7.1; N, 2.0. *Calcd.* for C₉₀H₁₀₀B₂N₂OP₄Co: C, 75.58; H, 7.05; N, 1.96%. Found: C, 76.5; H, 7.1; N, 1.9. *Calcd.* for C₉₀H₉₈B₂N₂P₄Ni: C, 76.56; H, 6.99; N, 1.98%.

Physical Measurements

The electronic spectra were recorded on a Beckman DK2-A spectrophotometer in the solid state and on a Varian Cary Model 17 spectrophotometer in solution. The magnetic susceptibility value was measured with a Faraday balance.

X-Ray Data Collection

Crystallization yielded only very small crystals. The crystal selected for intensity measurements was one of the largest ones; its approximate dimensions

were 0.05 × 0.05 × 0.1 mm. It was mounted in a capillary at an arbitrary orientation. An Enraf-Nonius CAD 4 automatic diffractometer was used both for the determination of lattice parameters and for intensity data. The unit cell parameters were obtained by least-squares refinement of the setting angles for 25 reflections.

Crystal data

C₉₀H₁₀₀B₂N₂OP₄Co, $M = 1430.25$; triclinic, space group P1; $a = 13.252(2)$, $b = 13.943(2)$, $c = 24.316(5)$ Å, $\alpha = 70.660(14)$, $\beta = 75.219(14)$, $\gamma = 69.231(13)^\circ$, $U = 3915.17$ Å³; $Z = 2$; $D_c = 1.21$ g cm⁻³; $F(000) = 1518$; $\mu(\text{MoK}\alpha) = 1.55$ cm⁻¹.

Mo-K α radiation ($\lambda = 0.7093$ Å) monochromatized by a graphite crystal was used to measure the intensities of 7277 independent reflections in the range $2 < \theta < 20^\circ$ with the θ - 2θ scan technique. A total of 1403 reflections with intensity greater than $2\sigma(I)$ were considered observed and used for the structure solution and refinement. The standard deviation of the intensity was calculated as follows: $\sigma(I) = [S^2(C + R^2B) + (fI)^2]^{1/2}$, $I = S(C - RB)$, where S is the scan rate, C is the total integrated peak count, R is the ratio of scan time to background counting time (2.0 in this case), B is the total background count and the parameter f is a factor introduced to downweight intense reflections. Here f was set to 0.03.

Intensities were corrected for Lorentz polarization effects; absorption corrections were not applied.

Structure Solution and Refinement

The position of the cobalt atom was determined from a Patterson synthesis. Additional Fourier maps showed all the atoms of the macrocycle and of the two tetraphenylborate counterions contained in the asymmetric unit. In least-squares calculations the function minimized was $\sum w(|F_o| - |F_c|)^2$. Unit weights were used throughout the refinement. Because of the great number of independent parameters, blocked full-matrix least-squares refinement was used, dividing the structure in the following four blocks:

- 1) cobalt, oxygen, and two phosphorus atoms together with the two phenyl rings bonded to them plus half of the atoms in the macrocycle;
- 2) the other two phosphorus atoms with the respective phenyl rings plus the remaining atoms of the macrocycle;
- 3) a tetraphenylborate anion;
- 4) the second tetraphenylborate anion.

All the benzene rings in the structure were refined as rigid groups. Initially isotropic temperature factors were used, but in the later refinement cycles anisotropic temperature factors were introduced for the atoms in the coordination sphere of the metal; this

TABLE I. Fractional Atomic Coordinates and Anisotropic Thermal Parameters^a ($\times 10^4$), with e.s.d.'s in parentheses, for [Co(H₂O)(γ -[18]aneP₄N₂)] [BPh₄]₂.

Atom	<i>x/a</i>	<i>y/b</i>	<i>z/c</i>	<i>U</i> ₁₁	<i>U</i> ₂₂	<i>U</i> ₃₃	<i>U</i> ₁₂	<i>U</i> ₁₃	<i>U</i> ₂₃
Co	1784(4)	3145(4)	2383(2)	523(33)	659(35)	477(33)	-283(28)	1(26)	-189(25)
P(1)	2715(7)	3354(7)	1454(4)	808(82)	697(81)	606(76)	-341(65)	-119(63)	-168(62)
P(2)	3400(7)	1956(7)	2632(4)	465(69)	570(63)	614(66)	-158(54)	-106(52)	-227(50)
P(3)	793(6)	2748(6)	3303(3)	599(67)	426(62)	559(64)	-227(53)	-141(53)	-10(48)
P(4)	66(7)	3809(7)	2118(3)	612(69)	776(73)	501(65)	-355(58)	-92(53)	-59(54)
O _w	2290(14)	4504(14)	2432(8)	561(140)	723(154)	1059(173)	-250(120)	-41(122)	-532(131)

^aThe anisotropic parameters are of the form $\exp(-2\pi^2(h^2a^{*2}U_{11} + k^2b^{*2}U_{22} + l^2c^{*2}U_{33} + 2hka^*b^*U_{12} + 2hla^*c^*U_{13} + 2klb^*c^*U_{23}))$.

TABLE II. Fractional Atomic Coordinates and Isotropic Thermal Parameters ($\times 10^4$), with e.s.d.'s in parentheses, for [Co(H₂O)-(γ -[18]aneP₄N₂)] [BPh₄]₂.

Atom	<i>x/a</i>	<i>y/b</i>	<i>z/c</i>	<i>U</i> (Å ²)
N(1)	2623(17)	2651(17)	3951(9)	512(67)
N(2)	529(20)	5511(18)	961(10)	810(83)
C(1)	4169(21)	3078(21)	1513(11)	544(89)
C(2)	4508(20)	1923(20)	1962(11)	462(85)
C(3)	4178(21)	2086(20)	3137(12)	510(86)
C(4)	363(22)	1846(21)	3786(12)	525(87)
C(5)	1768(20)	2159(20)	4322(11)	471(84)
C(6)	1303(21)	1694(20)	3956(11)	534(88)
C(7)	-198(19)	2188(19)	3176(10)	385(78)
C(8)	431(20)	2631(20)	2528(11)	562(90)
C(9)	-234(23)	3983(23)	1377(13)	764(103)
C(10)	-479(24)	5199(24)	988(13)	814(108)
C(11)	1535(23)	4971(21)	589(12)	580(92)
C(12)	2517(21)	4664(20)	880(11)	547(91)
C(13)	2762(17)	2429(13)	1068(9)	658(98)
C(131)	2092(17)	1764(13)	1289(9)	540(89)
C(132)	2138(17)	1060(13)	982(9)	744(102)
C(133)	2855(17)	1019(13)	453(9)	673(98)
C(134)	3525(17)	1684(13)	232(9)	788(105)
C(135)	3479(17)	2388(13)	539(9)	848(111)
C(14)	3406(19)	557(12)	2888(7)	459(84)
C(141)	4316(19)	-250(12)	3094(7)	919(117)
C(142)	4343(19)	-1313(12)	3238(7)	1208(138)
C(143)	3459(19)	-1569(12)	3176(7)	611(93)
C(144)	2548(19)	-762(12)	2970(7)	697(99)
C(145)	2522(19)	301(12)	2826(7)	632(95)
C(15)	-31(16)	3847(13)	3628(7)	434(80)
C(151)	447(16)	4587(13)	3635(7)	567(89)
C(152)	-125(16)	5347(13)	3948(7)	712(100)
C(153)	-1174(16)	5367(13)	4254(7)	805(107)
C(154)	-1652(16)	4627(13)	4247(7)	878(100)
C(155)	-1080(16)	3867(13)	3934(7)	615(92)
C(16)	-936(16)	4953(12)	2531(17)	478(83)
C(161)	-620(16)	5787(12)	2380(7)	608(93)
C(162)	-1410(16)	6688(12)	2514(7)	888(113)
C(163)	-2515(16)	6756(12)	2619(7)	750(102)
C(164)	-2831(16)	5922(12)	2591(7)	856(109)
C(165)	-2041(16)	5020(12)	2457(7)	829(106)

(continued overleaf)

TABLE II. (continued)

Atom	x/a	y/b	z/c	$U (\text{Å}^2)$
C(17)	2757(21)	3345(21)	4281(12)	586(89)
C(18)	3549(22)	3976(22)	3872(12)	657(94)
C(19)	3549(25)	4801(25)	4214(13)	937(113)
C(20)	271(16)	6745(26)	844(15)	1010(119)
C(21)	-89(29)	7321(31)	241(17)	1320(146)
C(22)	-205(31)	8547(33)	201(17)	1527(161)
C(23)	4246(13)	7010(16)	672(6)	525(86)
C(231)	3845(13)	8090(16)	395(6)	684(95)
C(232)	3446(13)	8408(16)	-135(6)	808(103)
C(233)	3446(13)	7646(16)	-390(6)	635(93)
C(234)	3846(13)	6566(16)	-113(6)	551(87)
C(235)	4246(13)	6248(16)	418(6)	447(80)
C(24)	3327(13)	6735(13)	1849(8)	460(83)
C(241)	2333(13)	7028(13)	1651(8)	657(95)
C(242)	1357(13)	7182(13)	2046(8)	834(105)
C(243)	1376(13)	7042(13)	2639(8)	852(107)
C(244)	2370(13)	6748(13)	2837(8)	637(94)
C(245)	3346(13)	6595(13)	2442(8)	586(91)
C(25)	5118(19)	7528(14)	1414(8)	599(91)
C(251)	6241(19)	7383(14)	1302(8)	708(97)
C(252)	6639(19)	8179(14)	1310(8)	838(106)
C(253)	5914(19)	9122(14)	1428(8)	927(111)
C(254)	4791(19)	9627(14)	1539(8)	887(110)
C(255)	4393(19)	8471(14)	1532(8)	770(101)
C(26)	5435(12)	5409(11)	1502(9)	503(84)
C(261)	5326(12)	4618(11)	2026(9)	557(90)
C(262)	6099(12)	3616(11)	2104(9)	578(91)
C(263)	6981(12)	3405(11)	1659(9)	503(83)
C(264)	7090(12)	4195(11)	1135(9)	577(91)
C(265)	6317(12)	5197(11)	1057(9)	505(86)
C(27)	7155(14)	9076(14)	3975(8)	470(82)
C(271)	7350(14)	8173(14)	3788(8)	610(90)
C(272)	6617(14)	7574(14)	4003(8)	729(99)
C(273)	5687(14)	7876(14)	4406(8)	742(100)
C(274)	5491(14)	8779(14)	4594(8)	732(98)
C(275)	6225(14)	9378(14)	4378(8)	790(103)
C(28)	8425(21)	9933(14)	3001(6)	712(99)
C(281)	9512(21)	9856(14)	2749(6)	638(94)
C(282)	9826(21)	9998(14)	2142(6)	968(118)
C(283)	9053(21)	10215(14)	1786(6)	934(112)
C(284)	7966(21)	10291(14)	2038(6)	1034(121)
C(285)	7652(21)	10150(14)	2646(6)	951(118)
C(29)	9213(11)	9035(15)	4063(7)	308(74)
C(291)	9600(11)	7931(15)	4169(7)	661(94)
C(292)	10545(11)	7363(15)	4424(7)	848(107)
C(293)	11103(11)	7900(15)	4573(7)	796(102)
C(294)	10715(11)	9005(15)	4467(7)	772(103)
C(295)	9770(11)	9572(15)	4213(7)	723(99)
C(30)	7510(13)	10941(13)	3913(10)	649(93)
C(301)	7149(13)	11872(13)	3476(10)	664(94)
C(302)	6679(13)	12844(13)	3618(10)	790(102)
C(303)	6570(13)	12886(13)	4196(10)	688(96)
C(304)	6931(13)	11956(13)	4633(10)	708(98)
C(305)	7401(13)	10983(13)	4491(10)	611(91)

lowered the agreement factor R to the final value of 0.0692. In the final cycle of least-squares refinement the shifts on all refined parameters were well

below the standard deviations. The limited amount of observed data precluded anisotropic refinement of the other non-hydrogen atoms in the asymmetric

TABLE III. Interatomic Distances (Å) and Angles (°), with e.s.d.'s in parentheses, for [Co(H₂O)(γ-[18]aneP₄N₂)] [BPh₄]₂.

Bond Distances

Cobalt(II) Complex

Co–P(1)	2.259(9)
Co–P(2)	2.276(9)
Co–P(3)	2.288(8)
Co–P(4)	2.304(10)
Co–O _w	2.269(24)

Macrocycle

P(1)–C(1)	1.861(30)	N(1)–C(17)	1.523(45)
P(1)–C(12)	1.874(24)	N(2)–C(10)	1.526(48)
P(1)–C(13)	1.807(27)	N(2)–C(11)	1.511(34)
P(2)–C(2)	1.895(24)	N(2)–C(20)	1.570(43)
P(2)–C(3)	1.878(36)	C(1)–C(2)	1.600(32)
P(2)–C(14)	1.838(19)	C(3)–C(4)	1.539(36)
P(3)–C(6)	1.855(24)	C(5)–C(6)	1.592(49)
P(3)–C(7)	1.877(33)	C(7)–C(8)	1.557(37)
P(3)–C(15)	1.828(19)	C(9)–C(10)	1.607(39)
P(4)–C(18)	1.864(29)	C(17)–C(18)	1.552(40)
P(4)–C(9)	1.863(35)	C(18)–C(19)	1.625(55)
P(4)–C(16)	1.827(18)	C(20)–C(21)	1.526(52)
N(1)–C(4)	1.472(31)	C(21)–C(22)	1.633(66)
N(1)–C(5)	1.479(34)		

Tetraphenylborate Counterions

B(1)–C(23)	1.759(38)	B(2)–C(27)	1.718(42)
B(1)–C(24)	1.763(34)	B(2)–C(28)	1.700(34)
B(1)–C(25)	1.656(50)	B(2)–C(29)	1.669(34)
B(1)–C(26)	1.652(31)	B(2)–C(30)	1.693(38)

Bond Angles

Cobalt(II) Complex

P(1)–Co–P(2)	84.0(3)	P(2)–Co–P(4)	159.8(5)
P(1)–Co–P(3)	172.3(5)	P(2)–Co–O _w	91.2(5)
P(1)–Co–P(4)	96.2(4)	P(3)–Co–P(4)	81.5(3)
P(1)–Co–O _w	87.2(5)	P(3)–Co–O _w	100.6(5)
P(2)–Co–P(3)	95.6(3)	P(4)–Co–O _w	109.0(5)

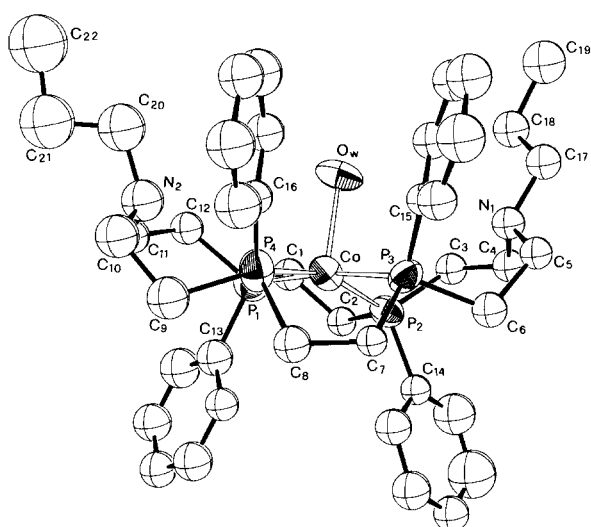
Macrocycle

Co–P(1)–C(1)	106.7(9)	C(8)–P(4)–C(9)	98.2(15)
Co–P(1)–C(12)	123.6(9)	C(8)–P(4)–C(16)	106.9(10)
Co–P(1)–C(13)	116.3(8)	C(9)–P(4)–C(16)	103.5(11)
C(1)–P(1)–C(12)	99.1(13)	P(1)–C(1)–C(2)	106.0(19)
C(1)–P(1)–C(13)	103.9(12)	P(1)–C(12)–C(11)	113.3(22)
C(12)–P(1)–C(13)	104.3(12)	P(2)–C(2)–C(1)	105.7(15)
Co–P(2)–C(2)	111.2(8)	P(2)–C(3)–C(4)	112.5(22)
Co–P(2)–C(3)	123.8(9)	P(3)–C(6)–C(5)	110.2(18)
Co–P(2)–C(14)	114.7(9)	P(3)–C(7)–C(8)	112.2(18)
C(2)–P(2)–C(3)	98.0(13)	P(4)–C(8)–C(7)	112.2(23)
C(2)–P(2)–C(14)	104.8(11)	P(4)–C(9)–C(10)	112.4(25)
C(3)–P(2)–C(14)	100.9(11)	N(1)–C(4)–C(3)	117.0(19)
Co–P(3)–C(6)	126.2(8)	N(1)–C(5)–C(6)	111.8(21)

(continued overleaf)

TABLE III. (continued)

Co-P(3)-C(7)	102.4(8)	N(1)-C(17)-C(18)	108.4(22)
Co-P(3)-C(15)	117.9(6)	N(2)-C(10)-C(9)	104.8(22)
C(6)-P(3)-C(7)	99.6(13)	N(2)-C(11)-C(12)	109.6(25)
C(6)-P(3)-C(15)	101.6(15)	N(2)-C(20)-C(21)	110.1(34)
C(7)-P(3)-C(15)	106.2(11)	C(4)-N(1)-C(5)	111.6(20)
Co-P(4)-C(8)	98.5(9)	C(4)-N(1)-C(17)	115.2(23)
Co-P(4)-C(9)	125.1(9)	C(5)-N(1)-C(17)	107.0(20)
Co-P(4)-C(16)	120.5(9)	C(10)-N(2)-C(11)	113.5(27)
C(10)-N(2)-C(20)	112.1(22)	C(17)-C(18)-C(19)	106.1(22)
C(11)-N(2)-C(20)	116.4(22)	C(20)-C(21)-C(22)	100.8(36)
<i>Tetraphenylborate Counterions</i>			
C(23)-B(1)-C(24)	103.4(20)	C(27)-B(2)-C(28)	105.3(25)
C(23)-B(1)-C(25)	107.9(19)	C(27)-B(2)-C(29)	109.7(18)
C(23)-B(1)-C(26)	108.7(23)	C(27)-B(2)-C(30)	107.7(17)
C(24)-B(1)-C(25)	109.3(22)	C(28)-B(2)-C(29)	110.2(18)
C(24)-B(1)-C(26)	112.8(19)	C(28)-B(2)-C(30)	111.3(18)
C(25)-B(1)-C(26)	114.0(23)	C(29)-B(2)-C(30)	112.4(26)

Fig. 2. ORTEP drawing of the complex cation $[\text{Co}(\text{H}_2\text{O})(\gamma\text{-[18]aneP}_4\text{N}_2)]^+$ with the atom labeling scheme.

unit. The ratio between the number of observed intensities and the number of independent parameters is $1403/290 = 4.8$. A difference electron density, calculated at $R = 0.0692$, showed several hydrogen atoms, both of the macrocycle and of the tetraphenylborate counterions, but their positions and temperature factors were not refined nor introduced in the structure-factor calculations.

All the calculations were performed with the SHELX-76 [7] set of programs, with coefficients for analytical approximation to the scattering factors and anomalous dispersion corrections from the International Tables [8]. Final atomic coordinates and

thermal parameters with estimated standard deviations obtained from the least-squares calculations are reported in Tables I–II.

Results and Discussion

The complex $[\text{Co}(\text{H}_2\text{O})(\gamma\text{-[18]aneP}_4\text{N}_2)] [\text{BPh}_4]_2$ exhibits a room temperature magnetic moment of 2.49 B.M., indicative of a low-spin electron configuration. The structure of this compound consists of discrete $[\text{Co}(\text{H}_2\text{O})(\gamma\text{-[18]aneP}_4\text{N}_2)]^{2+}$ cations and $[\text{BPh}_4]^-$ anions. Figure 2 reports an ORTEP drawing of the cation. Bond distances and angles are reported in Table III.

The cobalt atom is five-coordinate by the four phosphorus atoms of the ligand and by an oxygen atom of a water molecule. The coordination polyhedron around the cobalt atom is a markedly-distorted square-pyramid with the four phosphorus atoms forming the basal plane and the oxygen atom at the apex. The cobalt atom is displaced from the mean plane of the four phosphorus atoms by about 0.28 Å (see Table IV) towards the water molecule. The phosphorus atoms undergo a slight tetrahedral ruffling, being significantly displaced from their mean plane (see Table IV). The apical oxygen atom does not lie on the axis normal to this plane but is directed toward P(1) and P(2), presumably because of the steric interaction of the water molecule with the phenyl ring bonded to P(3) and a phenyl group of a tetraphenylborate anion. In fact, the oxygen atom makes close contacts with the carbon atoms belonging to these rings (3.30–3.40 Å).

TABLE IV. Least-Squares Plane Through the four Phosphorus Atoms, and Deviations of the Macrocycle Atoms from this Plane.

Equation of the plane in direct space:			
$6.0011x + 13.7793y + 10.7648z = 7.6928 \text{ \AA}$			
Deviations from the plane:			
P(1)	0.1233 \text{ \AA}	Co	0.2766 \text{ \AA}
P(2)	-0.1239	N(1)	1.7874
P(3)	0.1253	N(2)	1.2525
P(4)	-0.1247		

The Co–P distances range from 2.26 to 2.30 \text{ \AA} and are in agreement with the Co–P distances found in five-coordinated, low-spin complexes of cobalt(II) [1, 2, 9]. The Co–O distance of 2.27 \text{ \AA} appears to be rather long when compared with the Co–P distances, but it agrees with the usual values found for apical oxygen donors in square-pyramidal low-spin cobalt(II) complexes [1, 10].

The two nitrogen atoms of the ligand are not coordinated to the cobalt atom and lie on the same side of the phosphorus plane at distances of 4.036 and 4.170 \text{ \AA} from the cobalt atom. The macrocycle has a boat-shaped configuration, in contrast to the centrosymmetric, essentially planar arrangement assumed in the square-planar nickel analogue [3].

The solid $[\text{Co}(\text{H}_2\text{O})(\gamma\text{-[18]aneP}_4\text{N}_2)]\text{[BPh}_4\text{]}_2$ complex exhibits a ligand field spectrum, with band maxima at 6000 and 13000 cm^{-1} and a shoulder at 25.000 cm^{-1} , whose shape is typical of square-pyramidal low-spin cobalt(II) complexes [1, 11]. No significant spectral change is found in the methylcyanide solution, suggesting that the same stereochemistry also occurs in solution. The dibromide monohydrate analogue shows a reflectance spectrum (6000, 13200, 23700(sh) cm^{-1}) suggestive of square-pyramidal geometry. This is probably achieved by coordination of one water molecule in view of the close spectral similarity with the tetraphenylborate complex. In methylcyanide this dibromide complex behaves as a 1:1 electrolyte, indicating coordination of one bromide anion. The ligand field transitions show moderate blue-shifts with respect to the solid spectrum and a higher intensity of the second band in comparison to the first one (9600(ϵ , 28), 14600(ϵ , 41), 24700(sh) cm^{-1}). This can be considered, as being indicative of distortion towards trigonal-bipyramidal geometry [12].

As far as the nickel complexes are concerned, the spectrum of the solid $[\text{Ni}(\gamma\text{-[18]aneP}_4\text{N}_2)]\text{[BPh}_4\text{]}_2$ shows a broad symmetric band with a maximum at 24000 cm^{-1} , in agreement with its X-ray

square-planar structure [3]. For the dibromide analogue, on the contrary, the peak maximum falls at 21000 cm^{-1} , indicating interaction of nickel with one or two bromide anions [13]. When dissolved in methylcyanide, the tetraphenylborate complex behaves as a 2:1 electrolyte. Its absorption spectrum shows a broad band with the peak at 22600 cm^{-1} (ϵ , 1450). With respect to the spectrum of the square-planar solid, such a red shift suggests a five-coordinated structure due to solvent coordination [13].

The nickel dibromide complex acts as a 1:1 electrolyte in methylcyanide or methanol, supporting coordination of one bromide anion. The absorption spectrum in these solvents is also indicative of a low-spin, five-coordinated structure (21900 cm^{-1} , ϵ , 1400).

In conclusion, $\gamma\text{-[18]aneP}_4\text{N}_2$ acts toward cobalt and nickel as a tetradentate ligand both in the solid and in solution. Expansion of the metal coordination number is achieved by binding of a coordinating anion or of a solvent molecule, rather than by coordination of an amine group of the macrocycle. These results confirm the close interdependence between the coordinative behaviour of each macrocycle and its chiral configuration. Actually, molecular models show that this is a peculiar feature of $\gamma\text{-[18]aneP}_4\text{N}_2$ diastereoisomers, if all four phosphorus atoms are to be coordinated to the metal [2]. On the other hand, with the other isomers one or two E donor atoms of the macrocycle can be coordinated to the metal in addition to the four phosphorus atoms, according to the mutual chiralities of the phosphane groups.

Acknowledgements

We thank Mr. G. Vignozzi for microanalyses.

References

- 1 M. Ciampolini, P. Dapporto, N. Nardi and F. Zanobini, *J. Chem. Soc. Chem. Commun.*, 177 (1980); M. Ciampolini, P. Dapporto, A. Dei, N. Nardi and F. Zanobini, *Inorg. Chem.*, 21, 489 (1982).
- 2 M. Ciampolini, P. Dapporto, N. Nardi and F. Zanobini, *Inorg. Chem.*, 22, 13 (1983).
- 3 M. Ciampolini, N. Nardi, F. Zanobini, R. Cini and P. L. Orioli, *Inorg. Chim. Acta*, 76, L17 (1983).
- 4 M. Ciampolini, N. Nardi, P. Dapporto, P. Innocenti and F. Zanobini, *J. Chem. Soc., Dalton Trans.*, in press.
- 5 M. Ciampolini, N. Nardi, P. Dapporto and F. Zanobini, *J. Chem. Soc., Dalton Trans.*, in press.
- 6 P. Dapporto, M. Ciampolini, N. Nardi and F. Zanobini, *Inorg. Chim. Acta*, 76, L153 (1983).

- 7 G. M. Sheldrick, 'SHELX-76, Program for Crystal Structure Determination', Cambridge University, 1976.
- 8 'International Tables for X-Ray Crystallography', Kynoch Press, Birmingham, England, 1974, Vol. 4.
- 9 M. Di Vaira, S. Midollini and L. Sacconi, *Inorg. Chem.*, **16**, 1518 (1977).
- 10 G. J. Bullen, *Acta Crystallogr.*, **12**, 703 (1959);
G. W. Roberts, S. C. Cummings and J. A. Cunningham, *Inorg. Chem.*, **15**, 2503 (1976).
- 11 R. L. Carlin, *Trans. Met. Chem.*, **1**, 1 (1965);
C. Daul, C. W. Schläpfer and A. Zelewsky, *Struct. Bonding (Berlin)*, **36**, 129 (1979).
- 12 J. K. Stalik, P. W. Corfield and D. W. Meek, *Inorg. Chem.*, **12**, 1668 (1973);
Y. Nishida and H. Shimohori, *Bull. Chem. Soc. Japan*, **46**, 2406 (1973).
- 13 C. Furlani, *Coord. Chem. Rev.*, **3**, 141 (1968).